Structure and propagation of modes of large mode area holey fibers

J.C. Gates, C.W.J. Hillman, Joanne C. Baggett, K. Furusawa, Tanya M. Monro, and W.S. Brocklesby

Optoelectronics Research Centre, University of Southampton, Southampton, SO17 1BJ UK
wsb@orc.soton.ac.uk

Abstract: We report cross-section measurement and propagation measurement of modes of large mode area holey fibers using near-field scanning optical microscopy (NSOM). Mode profiles are measured at the fiber end face using a scanning optical fiber tip held 10 nm from the surface, and compared to theoretical models. Both amplitude and phase of the electric field of the propagating light is measured using NSOM techniques as a function of distance from the fiber end, from 10 nm to 150 μm. Good agreement is found between the data and simple scalar paraxial beam propagation simulations of theoretical mode profiles.

OCIS codes: (060.2270) Fiber characterization, (110.0180) Microscopy

References and links

1. J.C.Baggett, T.M.Monro, K.Furusawa, D.J.Richardson, "Comparative study of large mode holey and conventional fibers," Opt. Lett. **26** 1045-1047 (2001).
2. N. G. R. Broderick, T. M. Monro, P. J. Bennett & D. J. Richardson. "Nonlinearity in holey optical fibers: measurement and future opportunities," Opt. Lett. **24**, 1395-1397 (1999).
3. T. A. Birks, D. Mogilevtsev, J. C. Knight & P. S. Russell, "Dispersion compensation using single-material fibers," IEEE Photonics Technol. Lett. **11**, 674-676 (1999).
4. T. M. Monro & D. J. Richardson, "Holey optical fibres: Fundamental properties and device applications," Comptes Rendus Physique **4**, 175-186 (2003).
5. T. M. Monro, D. J. Richardson, N. G. R. Broderick & P. J. Bennett, "Modeling large air fraction holey optical fibers," J. Lightwave Technol. **18**, 50-56 (2000).
6. K. Karrai & R. D. Grober, "Piezoelectric Tip-Sample Distance Control for Near-Field Optical Microscopes," Appl. Phys. Lett. **66**, 1842-1844 (1995).
7. M. L. M. Balistreri, J. P. Korterik, L. Kuipers & N. F. van Hulst, "Local observations of phase singularities in optical fields in waveguide structures," Phys. Rev. Lett. **85**, 294-297 (2000).
8. J.C. Knight , T.A. Birks, R.F. Cregan, P.S. Russell, J.P. de Sandro, "Large mode area photonic crystal fibre," Electron. Lett. **4**, 1347-13 (1998).
9. G.P. Agrawal, *Nonlinear Fiber Optics* (Academic Press, 1989).
10. N.A. Mortensen & J.R. Folkenberg, "Near-field to far-field transition of photonic crystal fibers: symmetries and interference phenomena," Opt. Express **10** 475-481 (2002), http://www.opticsexpress.org/abstract.cfm?URI=OPEX-10-11-475

1. Introduction

Holey fibers have proved to be one of the most innovative areas of optical waveguide development in the recent past. Their guiding properties can be varied using geometrical rather than material parameters, and they can demonstrate some extreme variation of mode area [1], nonlinearity [2], and dispersion [3]. They are typically formed by drawing from a perform consisting of a large number of small capillaries, and the resultant structure can be very complex [4]. The electromagnetic modes which propagate in these structures are similarly much more complex than the modes of a traditional step-index fiber. As with other complex fiber structures, calculation of the form of holey fiber (HF) modes is typically done by numerical simulation [5].

#3704 - $15.00 US Received 27 January 2004; revised 23 February 2004; accepted 26 February 2004

In this paper we report the detailed measurement of HF modes at the end faces of the fibers using near-field scanning optical microscopy (NSOM). NSOM has several advantages over other mode measurement techniques. It allows resolution that is tip-aperture-limited for any evanescent fields at the end face, and diffraction-limited for propagating fields. It allows very accurate control of distance from the end face, via the piezoelectric scanning system used to control tip position, and can also measure the surface contour of the end face if the tip is locked to the surface via shear-force control [6]. These advantages make it an ideal tool for study of complex HF modes. In addition, because the tip measures the electric field at a particular position in space, cross-sectional profiles in any direction through the beam propagating away from the fiber end can be measured. Addition of an interferometer to the NSOM system [7] allows direct measurement of amplitude and phase of the electric field of the beam, instead of just intensity. This allows more direct comparison with propagation models of the beam from the end of the HF.

The combination of NSOM with interferometry allows us to characterize the mode profile of our fibers from the fiber end out through the Rayleigh region with high accuracy. In this letter we will present detailed measurements of the mode profiles as the beam propagates away from the end face of the fiber, and show that the propagation is modeled very well by a simple scalar beam propagation calculation, despite the complex nature of the HF mode.

2. Holey fibers

The fibers used in this work are silica, and the typical structure is shown in Fig. 1, with a hexagonal lattice of small holes except for one lattice point in the center, where the hole is missing. These fibers have the important properties that they can be single mode over large wavelength regimes, and their mode area is much larger than that of typical single mode step index fiber [8], making them ideally suitable for applications such as high-power low nonlinearity transmission. Although the holes shown in Fig. 1 have a regular hexagonal structure, the fiber guides via effective index rather than photonic crystal effects. In this paper the propagating modes of these fibers have been calculated using a hybrid orthogonal function method [5], which uses sums of Hermite polynomials to construct the field distribution, starting from the known refractive index profile of the fiber itself.

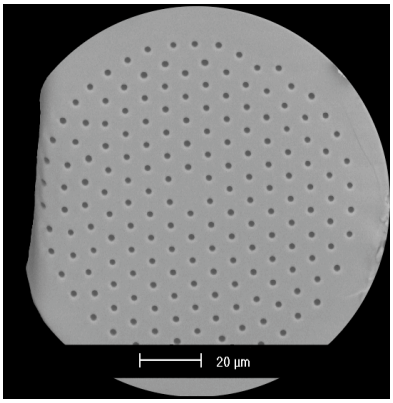

Fig 1. SEM image of end face of large mode area fiber

3. NSOM detection systems

The modal field of the HF were measured using a modification of a standard NSOM configuration. The laser sources at 633 nm or 1550 nm can be modulated, and the NSOM forms one arm of a fiber interferometer, in order to allow heterodyne measurement of phase and amplitude of the electric fields. The tip is formed from a drawn optical fiber, and coated in aluminum with a small (~80 nm) aperture at its end. The whole system is carefully

#3704 - $15.00 US Received 27 January 2004; revised 23 February 2004; accepted 26 February 2004

thermally isolated to stabilize the interferometer, which also allows the tip position to remain stable over long periods of time even when not in contact with the fiber end face. This system allows us to take cross-sections of the beam emerging from the end face in arbitrary planes relative to the end face itself. The accuracy of both the phase information and the absolute position of the tip are both dependent on good thermal stability. Over the course of a single scan, the phase may drift slowly by up to ~π/3 radians, and the absolute position by ~20nm in height and ~10nm laterally.

4. Experimental results

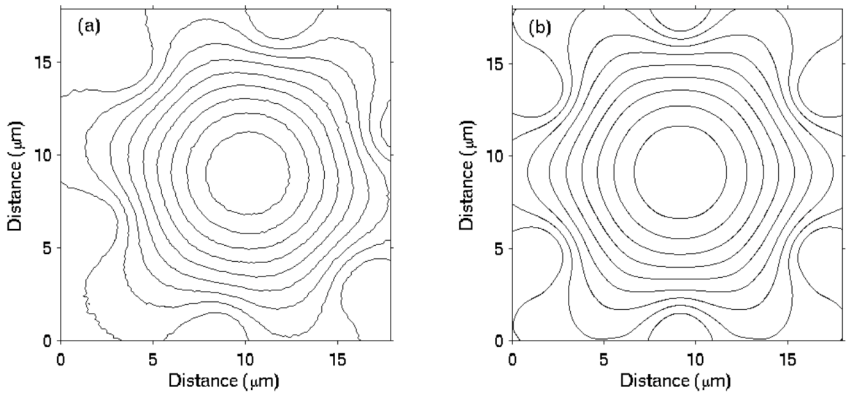

Fig. 2. Experimental (a) and theoretical (b) contour plots of the optical field amplitude 100nm above the fiber end face. Contours are linearly spaced, with spacing of 0.1. Maximum amplitude is scaled to 1. The rotation of the field in (a) is an experimental artifact.

Figure 2(a) shows the electric field amplitude measured in a plane 100 nm away from the end face of the large mode area fiber at 1550 nm. The contours are linearly spaced, with spacing of 0.1, and the maximum amplitude is scaled to 1. The confinement of the mode around the holes is clearly visible. Figure 2(b) shows the theoretically calculated mode, based on knowledge of the glass structure, with equivalent contour lines. The mode shapes correlate well, although the mode field area is overestimated by the theoretical calculations. Cross-sections across the mode profiles are shown in Fig. 3. The form of the cross-sections agrees well, but the widths from measured and theoretical mode field profiles differ by ~5-10%. The glass used to fabricate this fiber has been observed to have inhomogeneities in its refractive index in the vicinity of the core, and this index variation, which is not included in the modeling, is likely to be responsible for the discrepancy.

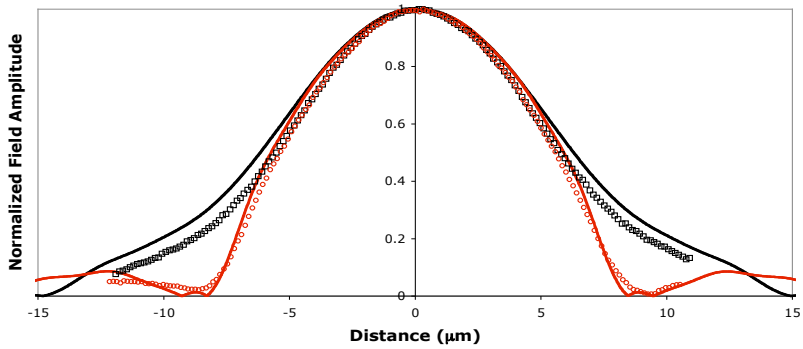

Fig. 3. Cross-sections across the optical field amplitude at the end face of the fiber. Red line is a cross-section of the theoretical mode across one of the inner ring of holes, and the red open circles are the equivalent data. Black line is a cross-section in an orthogonal direction, between the holes, and the black open squares are the equivalent data.

#3704 - $15.00 US Received 27 January 2004; revised 23 February 2004; accepted 26 February 2004

Figures 4 and 5 show cross-sections of the 1550nm beam emerging from the end face of the LMA fiber. The cross-sections are measured by first mapping the position of the end face of the fiber using shear force measurement, and then moving the tip in a plane perpendicular to the fiber end face. Distance from the centre of the fiber is shown on the x-axis of the figures. Figure 4 shows the intensity variation in a plane that crosses one of the innermost holes in the fiber, with the centre of the mode at 0 on the x axis. The scale is logarithmic to show detail of the low-intensity components. The intensity minimum at the hole is clearly visible. The high spatial frequencies in the beam cause diffraction at much higher angles than would be expected for a similar-area Gaussian mode.

Figure 5 shows a smaller-scale scan of the phase variation in a similar plane. In this figure the π phase shift between adjacent mode antinodes within the fiber gradually disappears as the mode propagates in free space. In both figures, the lower plot is a numerical simulation of the fields using a simple split-step beam propagation technique [9], which was used to simulate the propagation out of the end of the fiber, starting with the theoretically calculated modes. The agreement between the simulated and measured spatial variation is very good in both cases.

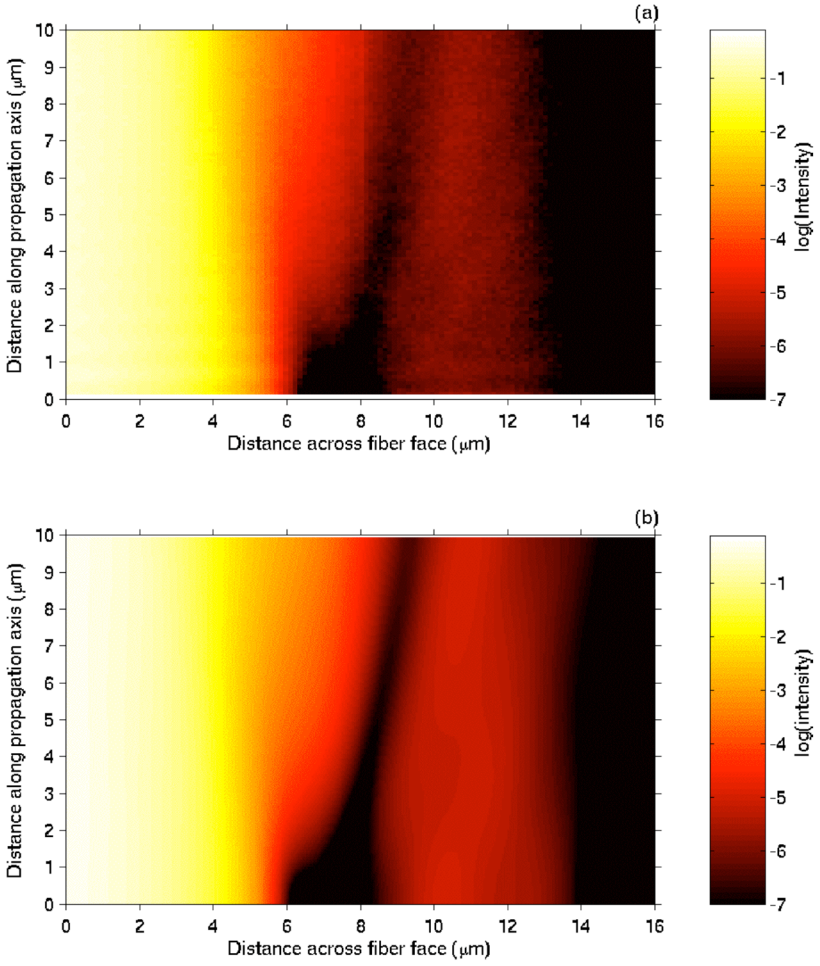

Fig. 4. Cross-section of the intensity of the mode as it propagates away from the end face of the fiber. The center of the mode is at the left end of the x-axis. The colormap scale is logarithmic, to show detail in the patterns. The top figure shows the square of the measured field amplitude, and the bottom figure shows the intensity distribution calculated by numerically propagating the theoretical mode.

#3704 - $15.00 US Received 27 January 2004; revised 23 February 2004; accepted 26 February 2004

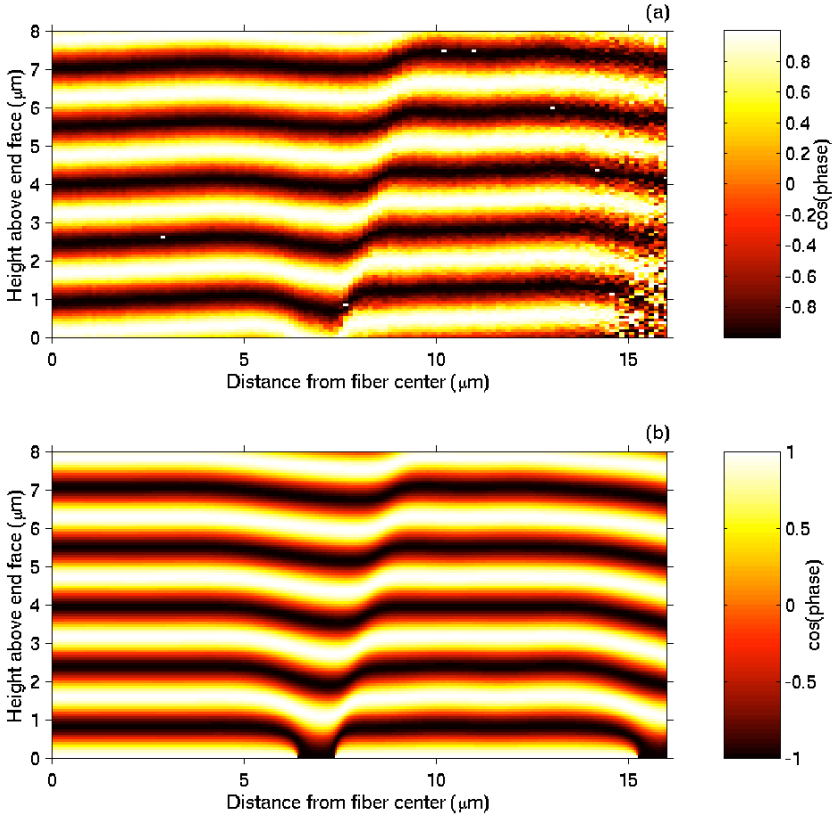

Fig 5. Cross-section of the phase of the mode as it propagates away from the end face of the fiber. The center of the mode is at the left end of the x-axis. The colormap scale shows the cosine of the phase. The top figure shows the measured phase, and the bottom figure shows the phase variation calculated by numerically propagating the theoretical mode. The phase offset is arbitrary.

As well as cross-sections along the propagation direction, it is possible to take cross-sections across the mode at different distances from the fiber end. Figure 6 shows the variation of the intensity of the mode as a function of distance out to 163 μm from the end face, equivalent to several Rayleigh lengths for a similar area Gaussian beam. The intensity scale is logarithmic, to show the low-intensity detail in the images. The wavelength in this case is 633 nm. Because of the large size of the mode compared to the travel on the stages used to control the tip, only about a quarter of the beam is shown in the figures. As the mode propagates away from the fiber end, the lobes appear to rotate by $\pi/6$ by a distance of 73 μm from the end face, and then rotate again by $\pi/6$ by the last frame, at 163 μm.

#3704 - $15.00 US Received 27 January 2004; revised 23 February 2004; accepted 26 February 2004

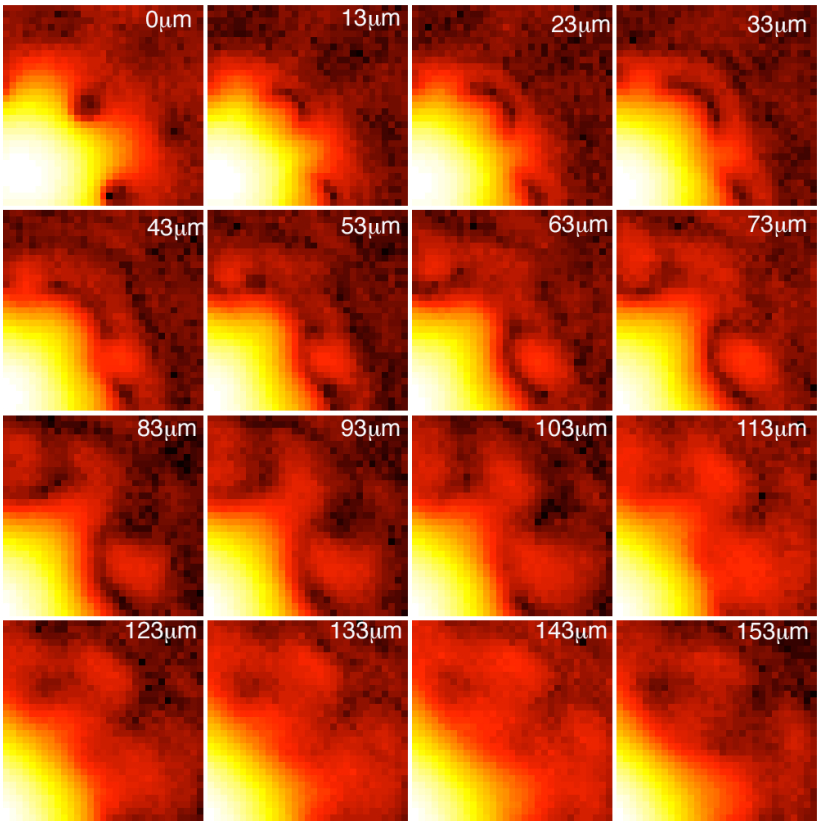

Fig. 6. Measured cross-sections of the intensity of the mode at longer distances from the fiber end face. Heights above the end face are shown on the figure. The top left frame is measured in contact with the end face, The intensity colormap scale is logarithmic to show low-intensity detail. The center of the mode is in the bottom left corner of each frame.

5. Conclusions

We have shown that techniques originally developed for NSOM can be used very effectively to measure the modal field and propagation of light from holey fibers. The mode mapping at the end of the fiber produces results that compare well to the theoretically calculated modes, and provide advantages of traditional techniques, in that all spatial frequencies can be collected, and the maps can be directly related to the topographic structure of the fiber. The interferometric nature of the detection system, together with the heterodyne detection systems used, make it possible to collect maps of amplitude and phase, and the complex phase variation of the light as it exits the fiber end can be seen very clearly. Propagation over longer distances can be imaged directly, and the effects previously noted in photonic crystal fibers [10], of diffraction causing the position of the field lobes to appear to rotate as a function of distance from the fiber, can also be seen in these holey fibers. The behavior of the optical fields near the fiber end face can be modeled accurately in this case using a simple numerical technique using scalar fields, and the paraxial approximation. The SNOM-based measurement technique should be very effective when used on fibers with much more extreme geometries with much tighter confinement, where for example the modes in the fiber may have dimensions which are less than the wavelength in air. The advantages over traditional measurement techniques will be even more obvious in these extreme geometries.

#3704 - $15.00 US Received 27 January 2004; revised 23 February 2004; accepted 26 February 2004